STEM CELLS

TISSUE-SPECIFIC STEM CELLS

DOT1L Activity Promotes Proliferation and Protects Cortical Neural Stem Cells from Activation of ATF4-DDIT3-Mediated ER Stress In Vitro

DEBORAH ROIDL,[a,b] NICOLE HELLBACH,[a] PATRICK P. BOVIO,[a,c] ALEJANDRO VILLARREAL,[a] STEFANIE HEIDRICH,[a] SIGRUN NESTEL,[d] BJÖRN A. GRÜNING,[e,f] ULRIKE BOENISCH,[g] TANJA VOGEL[a]

Key Words. Unfolded protein response • Cerebral cortex • Neural stem cells • Endoplasmic reticulum stress • Histone H3 methylation • H3K79

ABSTRACT

Growing evidence suggests that the lysine methyltransferase DOT1L/KMT4 has important roles in proliferation, survival, and differentiation of stem cells in development and in disease. We investigated the function of DOT1L in neural stem cells (NSCs) of the cerebral cortex. The pharmacological inhibition and shRNA-mediated knockdown of DOT1L impaired proliferation and survival of NSCs. DOT1L inhibition specifically induced genes that are activated during the unfolded protein response (UPR) in the endoplasmic reticulum (ER). Chromatin-immunoprecipitation analyses revealed that two genes encoding for central molecules involved in the ER stress response, *Atf4* and *Ddit3* (*Chop*), are marked with H3K79 methylation. Interference with DOT1L activity resulted in transcriptional activation of both genes accompanied by decreased levels of H3K79 dimethylation. Although downstream effectors of the UPR, such as *Ppp1r15a/Gadd34, Atf3*, and *Tnfrsf10b/Dr5* were also transcriptionally activated, this most likely occurred in response to increased ATF4 expression rather than as a direct consequence of altered H3K79 methylation. While stem cells are particularly vulnerable to stress, the UPR and ER stress have not been extensively studied in these cells yet. Since activation of the ER stress program is also implicated in directing stem cells into differentiation or to maintain a proliferative status, the UPR must be tightly regulated. Our and published data suggest that histone modifications, including H3K4me3, H3K14ac, and H3K79me2, are implicated in the control of transcriptional activation of ER stress genes. In this context, the loss of H3K79me2 at the *Atf4*- and *Ddit3*-promoters appears to mark a point-of-no-return that activates the death program in NSCs. STEM CELLS *2016;34:233–245*

SIGNIFICANCE STATEMENT

Posttranslational histone modification control gene expression. They are means to pass on transcriptional information from one cell generation to another. We describe the impact of histone H3 dimethylation at lysine 79 (H3K79me2) in neural stem cells. Inhibiting the enzymatic activity mediating this modification leads to cell division defects and cell death by controlling expression of central transcription factors implicated in stress response. Histone methylations are a way to balance how stem cells can cope with the activation of the stress response, which can range from proliferation to differentiation and, in case of H3K79me2, to the control of cell death.

INTRODUCTION

DOT1L (DOT1-like, histone H3 methyltransferase/KMT4) methylates histone H3 at position lysine 79 and it is responsible for mono- (H3K79me1), di- (H3K79me2), and trimethylation (H3K79me3). H3K79 methylation is conserved from yeast to humans but it mediates different cellular effects. In yeast, Dot1 is implicated in telomeric silencing [1], and in global genomic repair [2]. Mammalian DOT1L facilitates recruitment of TRP53BP1 (transformation related protein 53 binding protein 1) to DNA double-strand-breaks (DSBs), and initiates the repair process as well as transcription after UV-damage induced DSBs [3, 4]. DOT1L is also implicated in cell-cycle-control. In this context, DOT1L is required for the correct assembly of the centrosome and mitotic spindle, and also regulates cell cycle progression into S-phase through repression of genes for various cyclin-dependent kinase inhibitor proteins in cancer cells [5]. Mitosis in various organ systems and meiosis are both affected in conditions of

[a]Department of Molecular Embryology, Institute of Anatomy and Cell Biology, Albert-Ludwigs-University, Freiburg, Freiburg, Germany; [b]Hermann Staudinger Graduate School, Albert-Ludwigs-University, Freiburg, Freiburg, Germany; [c]Faculty of Biology, Albert-Ludwigs-University, Freiburg, Freiburg, Germany; [d]Department of Neuroanatomy, Institute of Anatomy and Cell Biology, Albert-Ludwigs-University, Freiburg, Freiburg, Germany; [e]Bioinformatics Group, Department of Computer Science, Albert-Ludwigs-University, Freiburg, Freiburg, Germany; and [f]Pharmaceutical Bioinformatics, Institute of Pharmaceutical Science, Albert-Ludwigs-University Freiburg, Freiburg, Germany; [g]Deep Sequencing Facility, Max Planck Institute of Immunobiology and Epigenetics, Freiburg, Germany

Correspondence: Tanja Vogel, Ph.D., Department of Molecular Embryology, Institute of Anatomy and Cell Biology, Albert-Ludwigs-University Freiburg, Albertstr. 17, 79104 Freiburg, Germany. Telephone: + 49-761-203-5086; Fax: + 49-761-203-5091; e-mail: tanja.vogel@anat.uni-freiburg.de

Received April 23, 2015; accepted for publication August 7, 2015; first published online in STEM CELLS *EXPRESS* August 24, 2015.

1066-5099/2015/$30.00/0

//dx.doi.org/10.1002/stem.2187

impaired DOT1L function [6, 7]. Whether and to what extent DOT1L function and H3K79 methylation influence the proliferative capacity of embryonic stem cells (ESCs) is not entirely clear. Whereas the genetic deletion of DOT1L impairs proliferation, shRNA-mediated knockdown of DOT1L suggests that proliferation in undifferentiated mouse ESCs is not strictly dependent upon DOT1L function [8, 9]. However, when ESCs with shRNA-mediated knockdown of DOT1L are cultured in the presence of retinoic acid to induce differentiation, the cells respond with decreased proliferation, cell cycle arrest in G2/M-phase, and hyperploidy. Transcriptome analyses of these cells revealed altered expression of genes implicated in cell cycle control and proliferation [9]. Knockdown of DOT1L during cardiogenic differentiation of mouse ESCs results in a delayed expression of genes implicated in cardiomyocyte differentiation, although changes in cell proliferation and/or survival have not been reported [10]. Accordingly, hearts from mice with a cardiac-specific knockout of *Dot1l* display hypertrophic ventricles with reactive fibrosis, increased apoptosis, and intracellular vacuoles indicative of autophagy [11]. Furthermore, DOT1L deficiency also impairs differentiation, cell cycle progression, and survival during prenatal erythropoiesis [12]. Postnatally, DOT1L is also necessary for the maintenance of hematopoietic stem cells (HSCs) and lineage-specific hematopoietic progenitors [13]. In mixed lineage leukemia (MLL), MLL fusion proteins (e.g., MLL-AF9 (MLLT3)) aberrantly recruit DOT1L to promoters of transcription factors that maintain the proliferative state of HSCs. Deletion of DOT1L in this setting interferes with cell cycle progression as well, albeit there is no change in cell death rates [13]. In contrast, DOT1L deficiency in mouse intestinal stem cells revealed higher rates of apoptosis, although these cells had normal rates of proliferation, and the mice did not display any major phenotype [14]. DOT1L is also implicated in the reprogramming of human somatic cells. Inhibition of DOT1L induces transcription of pluripotency genes such as *NANOG* and *LIN28* during the generation of induced pluripotent stem cells from fibroblasts. In contrast to other DOT1L-deficient cells, these DOT1L-inhibited fibroblasts displayed no alterations in cell cycle profiles or cell survival [15]. Taken together, these studies indicate that one major function of DOT1L is to control proliferation, survival, and differentiation in a variety of stem cells, although its action might be context-dependent. The latter is illustrated by the finding that H3K79 methylation is associated with actively transcribed genes [16], but that it is also detectable at transcriptionally repressed loci [17, 18]. Since DOT1L has been purified as component of different protein complexes [19, 20], the network of interacting proteins might be responsible for controlling context-specific functions. Whereas DOT1L-RNA polymerase II complexes confer transcriptional activity, DOT1L-AF9 is implicated in transcriptional repression. H3K79 hypermethylation, mediated by AF9-DOT1L, is implicated in transcriptional repression of epithelial *ENaC*α (epithelial sodium channel) [18], and of *Tbr1* (T-box protein 1) during development of the cerebral cortex [17].

DOT1L has further important functions in nervous system-derived stem cells since patients presenting with neural tube defects (NTD) have decreased levels of H3K79 methylation [21]. Furthermore, the protein survival motor neuron (SMN) binds H3K79me1 and me2, and mutations of the *SMN1* gene are associated with spinal muscular atrophy [22].

The implications of H3K79 methylation in neurological diseases and the expression of DOT1L-interacting AF9 in neural stem cells (NSC) of the cerebral cortex prompted us to study the role of DOT1L in NSCs and central nervous system development in further detail. Here, we report that pharmacological inhibition of DOT1L activity in cortical-derived NSCs results in decreased cell proliferation and increased apoptosis. Our data reveal that the induction of a chronic endoplasmic reticulum (ER) stress response mainly activates the apoptotic pathway. Inactive DOT1L results in decreased H3K79me2 at the promoters of two central ER stress transcription factors *Atf4* and *Ddit3*. Activation of both is part of the downstream program of the unfolded protein response (UPR) that drives cells into apoptosis under conditions of prolonged and/or unresolved ER stress. Together, our data shed further light into the epigenetic mechanisms regulating the ER stress pathway in NSCs, and establish a link between ER stress and DOT1L-mediated H3K79me2.

Materials and Methods

Mice

All experiments with mice were carried out following European Communities Council Directive of November 24, 1986 (86/609/EEC) and approval of local authorities (X-11/09S, X14/04H).

Primary Cultures of NSCs

Cortical cells were isolated from embryonic NMRI mice at E14.5 and cultivated as described recently [23].

DOT1L Inhibitors

Five micromolar SGC0946 (gift from P. Brown) or where specifically indicated 1 μM, 5 μM, or 10 μM EPZ5676 (Active Biochemicals, Wanchai, Hong Kong) in dimethyl sulfoxide (DMSO) (Sigma-Aldrich, St. Louis, MO, USA) was applied to cortical cells after 4–5 hours at DIV (days in vitro) 0 and refreshed every second day. DMSO was used as control treatment.

Microarray Analysis

E14.5-derived cortical NSCs were treated with 5 μM SGC0946 and harvested at DIV3. Total RNA of treated and control samples from three independent experiments was isolated and hybridized to GeneChip Mouse Gene 2.0 ST Array (Affymetrix, Santa Clara, CA, USA).

Chromatin Immunoprecipitation-Sequencing

Cortical E14.5 NSCs from wild-type animals were isolated and directly fixed with 1% freshly prepared paraformaldehyde (PFA) (Roth, Karlsruhe, Germany) for 5 minutes at room temperature. Chromatin was sheared within 30 high-energy 30 seconds on and 30 seconds off cycles using Bioruptor Next Gen System (Diagenode, Seraing, Belgium). Ten micrograms of chromatin was incubated with either H3K79me2 antibody (2 μg, ab3594, Abcam, Cambridge, U.K.) or rabbit IgG (2 μg, C15410206, Diagenode, Seraing, Belgium) at 4 °C overnight. Immune complexes were washed with different buffers and DNA was extracted from the beads in 1% SDS/100 mM $NaHCO_3$. Reverse cross-linking was achieved by RNase A (Sigma-Aldrich, St. Louis, MO, USA) and subsequent Proteinase K (Roche, Basel, Switzerland) digestion. DNA samples were purified using MinElute Reaction Cleanup Kit and PCR purification

Kit (both Qiagen, Hilden, Germany). For library preparation NEB Next Ultra DNA Library Prep Kit for Illumina (NEB, Ipswich, MA, USA) was used to convert 10 ng immunoprecipitated DNA and input-DNA into indexed libraries for next-generation multiplex sequencing on the Illumina platform. Sequencing adaptors and PCR primers were from NEB (NEBNext Multiplex Oligos for Illumina, Index Primers Set 1 E7335, or Set 2 E7500S) (NEB, Ipswich, MA, USA). Samples were sequenced paired-end with a read length of 50 bp to the desired depth using Illumina's HiSeq2500. Detailed information is provided in Supporting Information Methods.

Chromatin Immunoprecipitation-Sequencing Data Analysis

Chromatin immunoprecipitation sequencing (ChIP-seq) reads were mapped to the mm9 genome assembly using Bowtie2 [24]. PCR duplicates were removed. Both ChIP-seq runs were merged and more than 65 million reads/sample analyzed. The genome was binned for read coverage of input and ChIP samples. The number of reads per bin was calculated and normalized to the total number of mappable reads (reads per kilobase per million, RPKM). Integrative genome viewer was used for enrichment visualization of the read coverages. MACS2 was applied for peak calling [25].

Statistics

Unpaired Student's *t* test, one sample *t* test, and one- or two-way ANOVA were applied, except for ChIP-seq and microarray analysis. Detailed information on the respective test used is provided with each experiment. Data are given as mean ± SEM, $n \geq 3$, *p*-value: *, $p < .05$; **, $p < .01$; ***, $p < .001$; ****, $p < .0001$.

Additional Material and Methods are in Supporting Information.

Results

Inhibition of DOT1L Activity in Primary Cortical NSCs Results in Impaired Proliferation, Survival, and Neuronal Differentiation

To assess the role of active DOT1L in mouse cortical NSCs we treated E14.5-derived cells with the substrate analog inhibitor, SGC0946 [26]. We verified via immunoblotting that this treatment resulted in a significant loss of H3K79me2 and me3 on a global level in total protein lysates (Fig. 1A, 1C). We further assessed whether inhibition of DOT1L activity and H3K79me2/3 might result in alterations of other histone modifications, for which association to H3K79me2/3 has been reported [8, 27]. However, we did not observe any global changes in H3K9me2, H4K20me3, and H2Bub, respectively (Fig. 1B, 1D). Next we analyzed the cellular response to DOT1L inhibition using real-time cell analyses (RTCA). As illustrated in Figure 1E, cell proliferation and/or survival were impaired after DOT1L inhibition compared to the control condition. We corroborated this finding using an shRNA-mediated knockdown of DOT1L (Fig. 1F). To discriminate whether cortical NSC proliferation and/or survival were dependent upon DOT1L function, we performed various immunocytochemistry (ICC) stainings. BrdU-pulsing of NSCs and subsequent anti-BrdU ICC staining revealed a significantly lower fraction of proliferating cells under conditions of DOT1L inhibition (Fig. 1G, 1I). We also observed more activated Caspase3 (CASP3)-positive cells after DOT1L inhibition (Fig. 1G, 1H, 1J). The decreased proliferation and increased apoptosis resulted in fewer numbers of HuC/D-positive neurons after 4 DIV (Fig. 1H, 1K). Propidium-iodide-based flow cytometry analyses corroborated our finding of increased cell death after DOT1L inhibition as indicated by a significant increase in cells in the sub-G1-fraction (Fig. 1L, 1M). Since DOT1L function might be important for transition from G2- to M-phase [7], we also assessed for specific changes in cell cycle parameters and observed fewer cells in the G2/M-fraction, but no significant changes in cell numbers in any of the other cell cycle phases, that is, G1 and S (Fig. 1M). Taken together we concluded from these data that DOT1L function is necessary for proliferation and survival of cortical NSCs during the neurogenic phase.

DOT1L Activity Prevents Transcriptional Induction of Metabolic and ER Stress Genes in Cortical NSCs

Epigenetic modification of histones is an important mechanism for transcriptional control and we rationalized that DOT1L activity will affect gene transcription in cortical NSCs. We addressed this question by analyzing changes in the transcriptome of E14.5-derived cortical NSCs following perturbation of DOT1L activity using microarray technology. From three independent experiments, we retrieved 27 genes with at least twofold altered expression levels with significant *p*-values ($p \leq .05$) (Fig. 2A). Most of the altered genes had increased expression, that is, 24 genes out of 27, indicating that DOT1L may mainly function to suppress gene transcription in cortical NSCs. This finding corroborated our earlier reported influence of DOT1L on *Tbr1*-transcription during cortical development [17]. Similar results were also obtained from intestinal tissue [14] and ESCs [9], in which deactivation of DOT1L resulted also in only a small number of transcriptionally altered genes. Using quantitative real-time PCR (qRTPCR) we corroborated the significant increase in gene transcription for 22 out of 24 upregulated and a significant decrease in one out of three downregulated candidates (Fig. 2B, dark blue and red bars). Gene ontology analysis of all 27 genes revealed that most of them were associated with metabolic processes, specifically lipid and steroid metabolism, cell death, and with the response to stress (Fig. 2C). In total, 11 genes were associated specifically with ER stress. We manually inspected the microarray data for further ER stress-related genes that might be altered after DOT1L inhibition, but which did not fulfill our initially applied stringent selection criteria. This analysis identified 10 additional genes that were changed upon DOT1L inhibition and associated with ER stress. We subsequently assessed the expression levels of all 21 ER stress-associated genes by qRTPCR with and without interference with DOT1L activity. Nineteen of these ER stress genes were significantly increased upon DOT1L inhibition (Fig. 2B, dark and light blue bars). Next, we assessed whether cortical NSCs experienced ER stress after shRNA-mediated knockdown of DOT1L. This analysis revealed six ER stress genes with significantly increased levels of transcription (Fig. 2D). In addition, overexpression of DOT1L resulted in decreased activity of seven ER stress genes (Fig. 2E), indicating that alteration of the ER stress-associated transcriptional program was indeed linked to DOT1L function.

To assess whether an altered ER-metabolism was also observable on a cellular level, we used electron microscopy

and assessed the morphology of DOT1L-inhibited and DMSO-treated NSCs. Inhibitor-treated cells showed clear signs of ER swellings, which were rarely identified in the control condition (Fig. 3Aa–3Ac). Quantification corroborated the finding of increased swollen ER as an indication of metabolic stress upon loss of DOT1L activity (Fig. 3B).

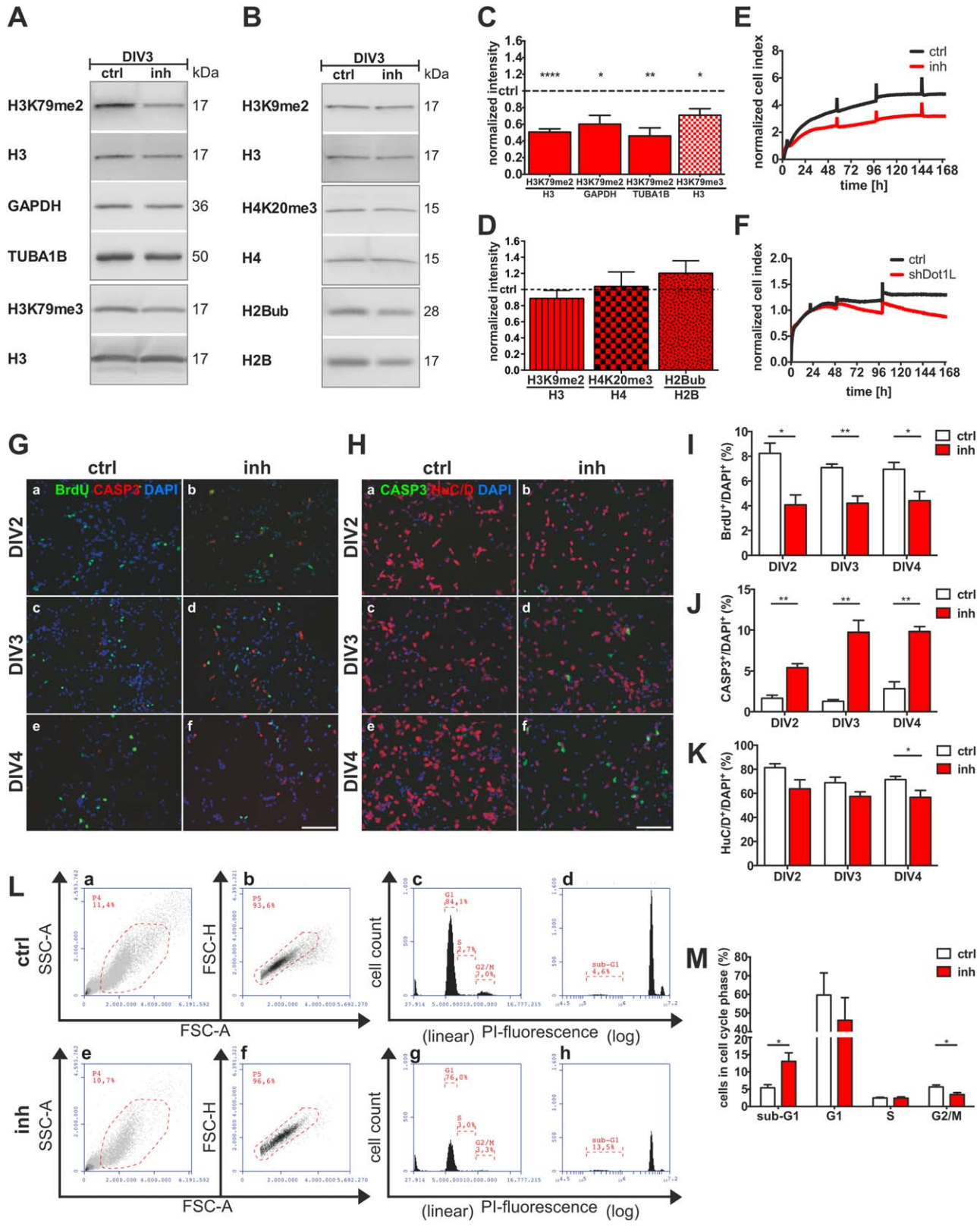

Figure 1.

Based on these data, we concluded that DOT1L activity is necessary to protect cortical NSCs from activation of a transcriptional program that results in ER stress. Consistently, DOT1L activity suppressed the activation of the *Atf* (*Activator of transcription*) *3/Atf4/Ddit* (*DNA-damage inducible transcript*) *3* transcription factor cascade.

Transcriptional Regulation of Metabolic and ER Stress Genes by DOT1L Is Cell-Type Specific

We next sought to analyze whether the role of DOT1L in suppressing the activation of the ER stress transcriptional program was also observed in different cell systems. To exemplarily investigate this, we treated mouse embryonic fibroblasts (MEF) as well as a human acute myeloid leukemia (AML) cancer cell line, MOLM-13, with the DOT1L inhibitor. MEFs were chosen as a well-established model system, which is widely used to study the roles of histone modifications. MOLM-13 cells were chosen as a leukemia disease model for which pharmacological DOT1L inhibition might serve as potential therapy [28]. DOT1L inhibition did not influence proliferation and/or survival of MEFs as indicated by RTCA analyses (Fig. 4A). Consistently, qRTPCR analyses revealed that the *Atf3/Atf4/Ddit3* transcription factor cascade was not activated. However, several of ER stress effectors involved in lipid or cholesterol biochemistry showed increased levels of transcription (Fig. 4B). Although MOLM-13 cells died after prolonged treatment with the DOT1L inhibitor, which is in accordance to published data (Fig. 4C), activation of ER stress genes did not appear to account for this cell death as assessed at DIV3 and 7 of inhibition (Fig. 4D, 4E). Therefore, we concluded that ER stress-induced cell death upon DOT1L inhibition might be cell type-specific and not a general hallmark of DOT1L activity.

Pharmacological inhibition of DOT1L entered phase I clinical trials as therapeutic strategy for treatment of specific types of leukemia. Here, a different DOT1L inhibitor, namely EPZ5676 [29], is used. We therefore tested whether treatment of cortical NSCs with EPZ5676 corroborated our findings using SGC0946. Figure 5 shows that different concentrations of EPZ5676 efficiently interfered with DOT1L-mediated H3K79me2 (Fig. 5A, 5B), and with cell proliferation and/or survival in a concentration-dependent manner in the RTCA assay (Fig. 5C). ICC revealed increased apoptosis (Fig. 5D, 5E) and little effect on neuronal differentiation (Fig. 5F). Application of EPZ5676 also induced transcription of the transcription factor cascade *Atf3/Atf4/Ddit3*, and of further ER stress-associated genes (Fig. 5G). We concluded that DOT1L inhibition activated ER stress in cortical NSCs independent from the different modes of inactivation (small molecule inhibitors, shRNA) and independent from a specific drug used in the assays (SGC0946 and EPZ5676).

DOT1L-Mediated H3K79me2 Is Enriched at Genes Involved in ER Stress and Suppresses Expression of the ER Stress-Associated Transcription Factors Atf4 and Ddit3

Next we used ChIP and subsequent sequencing (ChIP-seq) to uncover the distribution of H3K79me2 in the genome of E14.5-derived NSCs from wild-type forebrains. We specifically analyzed the H3K79me2 pattern at ER stress genes, which had an altered expression after DOT1L inhibition with SGC0946 in the previous experiments. We observed an enrichment of H3K79me2 at eight out of 21 analyzed genes including *Atf4, Ddit3, Ppp1r15a* (*protein phosphatase 1, regulatory* (*inhibitor*) *subunit 15A, Gadd34*), *Ero1l* (*ERO1-like*), *Nfe2l2* (*nuclear factor, erythroid derived 2, like 2, Nrf2*), *Tm7sf2* (*transmembrane 7 superfamily member 2*), *Lss* (*lanosterol synthase*), and *Mvd* (*mevalonate* (*diphospho*) *decarboxylase*) (Fig. 6Aa, 6Ab). The ChIP-seq profile indicated that H3K79me2 was distributed over the entire gene, ranging from the transcriptional start site (TSS) over the gene body to the transcriptional end site (TES). H3K79me2 peaked after the TSS and declined in the 3′ direction. We observed a slight enrichment of H3K79me2 in three genes, namely *Bcl2* (*B cell leukemia/lymphoma 2*), *Thbs1* (*thrombospondin 1*), and *Pck2* (*phosphoenolpyruvate carboxykinase 2*) (Fig. 6Ac). *Atf3, Eif4ebp1* (*eukaryotic translation initiation factor 4E binding protein 1*), *Chac1* (*ChaC, cation transport regulator 1*), *Tnfrsf10b* (*tumor necrosis factor receptor superfamily, member 10b*), *Slc7a11* (*solute carrier family 7* (*cationic amino acid transporter, y + system*), *member 11*), *Slc7a3, Stc2* (*stanniocalcin 2*), *Cav1* (*caveolin 1*), *Scd1* (*stearoyl-Coenzyme A desaturase 1*), and *Hmox1* (heme oxygenase 1) were not enriched for H3K79me2 compared to the input profile (Fig. 6Ad–6Af).

We concluded from these data that the majority of transcriptional changes that we observed after DOT1L inhibition were due to regulatory mechanisms other than alteration in H3K79me2, because only the transcription factors that initiate the ER stress response, *Atf4* and *Ddit3*, were clearly enriched for H3K79me2. We therefore analyzed whether known target genes of the transcription factors ATF4 and DDIT3 were

Figure 1. Interference with DOT1L activity in primary cortical neural stem cells (NSCs) resulted in impaired proliferation, survival, and differentiation. **(A, B)**: Immunoblot revealed specifically decreased H3K79me2 and me3 levels in E14.5-derived cortical NSCs after DOT1L inhibition. **(C, D)**: Densitometric quantification of (A) and (B). Statistical evaluation using one-sample *t* test with confidence level of 95% and hypothetical value of 1, $n = 3$–11 in (C), $n = 5$–8 in (D). **(E, F)**: Representative graphs of real-time cell analysis showing that inhibition of DOT1L activity (E) and shRNA-mediated knockdown of DOT1L (F), led to decreased proliferation and/or survival of E14.5-derived cortical NSCs. $n = 3$ for DOT1L inhibition, $n = 4$ for shRNA-mediated DOT1L-knockdown. **(G, H)**: Immunocytochemical stainings of BrdU-, activated Caspase3- (CASP3), and HuC/D-positive cells at different time intervals of treatments (DIV) under control (ctrl, DMSO) and DOT1L-inhibited (inh) condition. Scale bars = 100 μm. **(I–K)**: Quantification of cell numbers indicated reduced proliferation (BrdU) and increased cell death (CASP3) after interference with DOT1L activity. The number of positive cells was normalized to the total number of DAPI-positive cells. Unpaired Student's *t* test, $n = 3$–5. **(L)**: Representative graphs of flow cytometric analyses of PI stained cells showing that interference with DOT1L activity resulted in an increased number of cells in sub-G1- and decreased number of cells in G2/M-phase of the cell cycle. Upper panels display control condition, lower panels DOT1L-inhibitor-treated cells. (a, e): Panels display cells of interest gated in FSC-A/SSC-A dot blots. (b, f): FSC-A versus FSC-H plots to discriminate cell clumps. (c, g): Plots of the PI-fluorescence in a linear scale (linear) against side scatter (SSC-A) to quantify cells during G1-, S-, and G2/M-phase. (d, h): Plots of the PI-fluorescence in a logarithmic scale (log) against cell count (SSC-A) for quantification of cells in sub-G1-phase. **(M)**: Quantification of PI-stained cells present in different phases of the cell cycle. Inhibition of DOT1L activity in E14.5-derived cortical NSCs led to increased apoptosis as evidenced by the increased cell fraction in the sub-G1-peak. DOT1L inhibition led to fewer cells in G2/M-phase. Unpaired Student's *t* test, $n = 5$. *p*-Values: *, $p < .05$; **, $p < .01$; ****, $p < .0001$. Abbreviation: PI, propidium iodide.

among the genes that lacked enrichment of H3K79me2. Indeed, we revealed direct downstream targets of ATF4 and DDIT3, such as *Ppp1r15a, Ero1l, Bcl2, Atf3*, and *Tnfrsf10b* in the dataset. This suggested that DOT1L might be an upstream transcriptional regulator of the central stress response transcription factors *Atf4* and *Ddit3*. Their activation might have

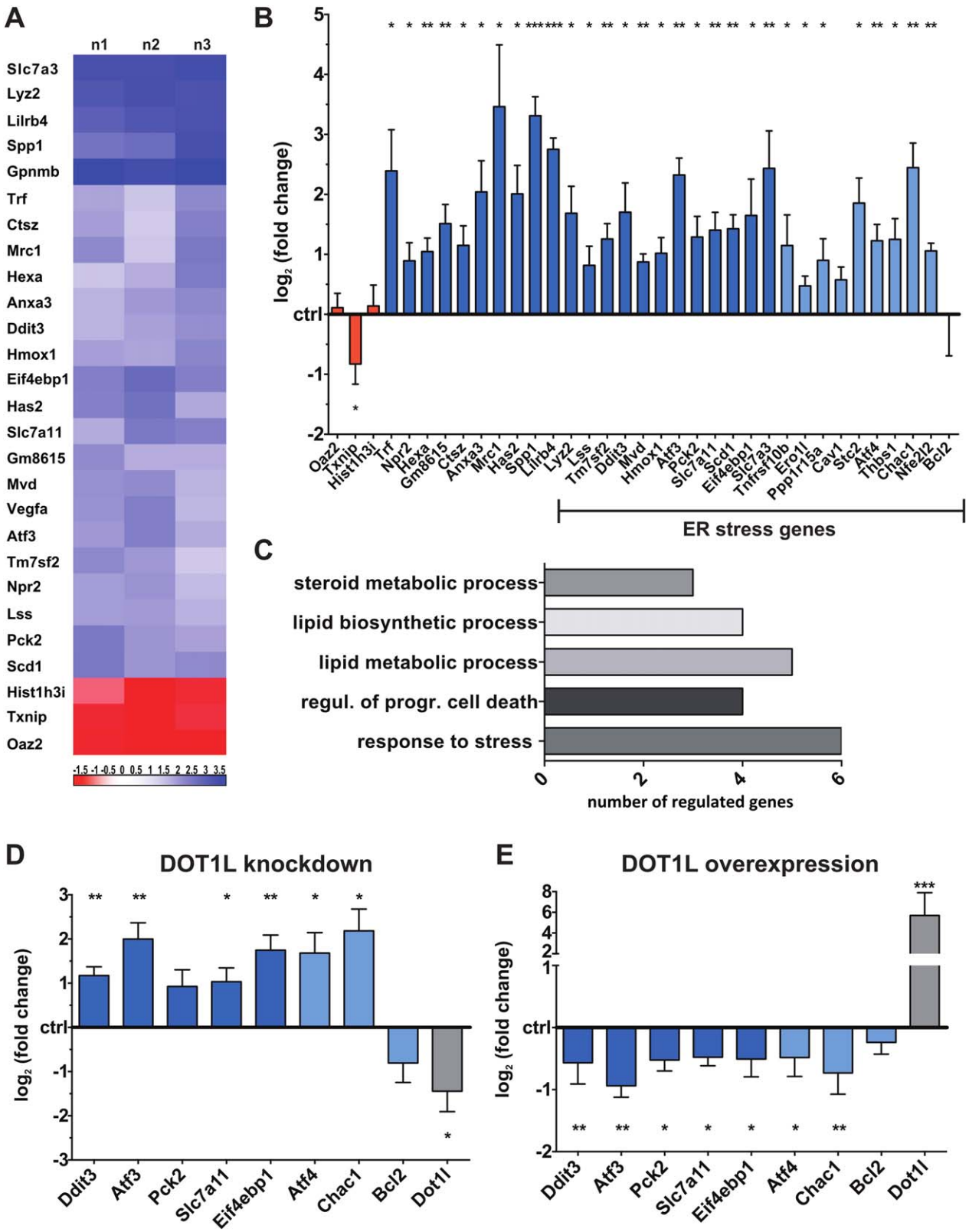

Figure 2.

led to a subsequent secondary initiation of the downstream transcriptional program that was mainly independent of DOT1L activity toward H3K79me2.

We subsequently tested the hypothesis that *Atf4* and *Ddit3* gene expression were dependent upon DOT1L activity, whereas other genes of the ER stress cascade, that is, *Atf3* and *Scd1*, were not. We determined the H3K79me2 enrichment for these selected genes without and after inhibition of DOT1L activity using ChIP followed by qRTPCR to assess H3K79me2 at different regions, that is, the TSS, gene body and TES, of *Atf4, Ddit3, Atf3*, and *Scd1*. Inhibition of DOT1L activity resulted in significantly decreased levels of H3K79me2 at *Atf4* and *Ddit3*. Our ChIP-seq profiles indicated a marginal enrichment of H3K79me2 at *Atf3* and *Scd1*, and in accordance with these data, H3K79me2 was less enriched at these genes as assessed by qRTPCR. As expected, we observed no changes after DOT1L inhibition (Fig. 6B), thereby corroborating our hypothesis that *Atf3* and *Scd1* transcription are independent of H3K79me2. Conversely, these data support that DOT1L-dependent H3K79me2 may directly suppress the expression of ER stress-associated transcription factors *Atf4* and *Ddit3*.

Chronic Inhibition of DOT1L Alters Transcription and Protein Levels of ER Stress-Associated Genes

Our data indicated that inhibiting DOT1L activity for 3 days in vitro resulted in apoptosis in response to the activation of the ER stress response transcriptional program. Inhibition of antiapoptotic BCL2 is one read-out of stress-induced cell death and DDIT3 has been reported to interfere with *Bcl2* transcription [30]. Our data did not suggest that *Bcl2* transcription was altered after inhibiting DOT1L activity (Fig. 2B, 2D, 2E). We therefore investigated BCL2 protein expression by immunoblotting and revealed that DOT1L inhibition resulted in reduced BCL2 levels (Fig. 7A, 7B). Cell death is the final response of a cell in case, that other processes of adaptation cannot compensate for the stress level. Thus, it reflects a response to chronic stress. To study whether DOT1L activity also prevents the early stress response, we investigated transcriptional changes of ER stress genes after shorter times of inhibition, that is, after 1 hour, 6 hours, and 24 hours. DOT1L inhibition resulted in significant transcriptional changes of *Atf4* and *Ddit3* only after 24 hours, whereas shorter treatment did not alter gene expression. Transcriptional induction of *Af4* was higher than that of *Ddit3* (Fig. 7C). At the protein level we observed that ATF4 expression was transiently and significantly increased after 24 hours of DOT1L inhibition but was unchanged in shorter or longer treatments (Fig. 7D, 7E). DOT1L inhibition for 1 hour up to 24 hours did not affect DDIT3, but DDIT3 protein levels significantly declined after 3 DIV. EIF4EBP1 protein levels declined and were significantly reduced after 3 days of DOT1L inhibition. This indicated a decline of protein synthesis after chronic DOT1L inhibition, which is generally associated with ER stress.

Taken together, our data revealed that chronic but not acute inhibition of DOT1L activity induced the transcriptional response to ER stress by increasing *Atf4* transcription and translation. This ultimately resulted in apoptosis, as reflected by downregulation of BCL2 and activation of downstream CASP3.

Discussion

Most of our reported observations on DOT1L function in NSCs are congruent with those in ESCs and other, committed stem cells, or progenitors. Generally, interference with DOT1L expression in stem cells results in decreased cell proliferation, increased apoptosis, and altered cell cycle distribution, either alone or in combination [8–14]. However, we detected a difference in the number of cells in G2/M-phase after DOT1L inactivation. This number was increased in ESCs [8] but decreased in NSCs. This difference might be due to a faster elimination/apoptosis of G2/M-phase arrested cells in NSCs cultures or reflect a context-dependent function of DOT1L. Context-dependent functions of DOT1L are emerging within recently published data, for example, during senescence. Whereas H3K79 hypomethylation might be attributed to senescence in aged rat lungs, brains of senescence-accelerated-prone mice revealed hypermethylation of H3K79 [7, 31]. Our data revealed further context-dependent functions of DOT1L as we discovered that NSCs specifically activate the chronic ER stress program that contributes to the observed cell death. However, DOT1L inactivation in MEFs and the leukemia cell line MOLM-13 did not result in the activation of ER stress genes. In particular, DOT1L acts differently

Figure 2. DOT1L inhibition induced transcription of metabolic and ER-stress genes in cortical neural stem cells (NSCs). **(A)**: Heatmap of genes with significantly altered transcription in E14.5-derived cortical NSCs after inhibition of DOT1L activity. Transcriptional changes from the mean of three experiments with *p*-values $< .05$, and values for the fold change smaller than -2 and higher than 2 were considered as significant. Twenty-four genes (blue) were transcriptional increased, three genes (red) decreased. Probe values were log 2 transformed. In order to identify differentially expressed genes between the groups, a one-way ANOVA in Partek was performed. Fisher's least significant difference was used as contrast method. Microarray dataset is deposited at the ArrayExpress (www.ebi.ac.uk/arrayexpress, Accession number A-GEOD-17408). **(B)**: Quantitative real-time PCR (qRTPCR) validation of expression changes after DOT1L inhibition, which were initially identified using microarray technology (red and dark blue bar), and of the extended transcriptome of ER stress genes, which did not fulfill initial selection criteria, but were considered to be putatively affected by DOT1L inhibition after manual inspection of microarray data (light blue bars). Given is the log 2-fold change for DOT1L-inhibited samples compared to DMSO-treated controls, indicating that interference with DOT1L activity resulted in increased transcription of ER stress genes. Unpaired Student's *t* test, $n = 3$–4. **(C)**: DAVID analyses of significantly regulated genes indicating that lipid metabolic and stress related genes were transcriptionally regulated through DOT1L activity. Given is the number of genes that falls into each of the categories. **(D)**: Knockdown of DOT1L in E14.5-derived cortical NSCs and validation of expression changes of genes involved in ER stress response using qRTPCR as in (B). Verification of knockdown of DOT1L was confirmed as well. Log 2 of the fold change is given compared to shScrambled-controls. $n = 3$. **(E)**: Overexpression of DOT1L led to decreased expression of ER stress genes as validated by qRTPCR. Verification of overexpression of DOT1L was confirmed via qRTPCR. Log 2 fold change is given compared to green fluorescent protein-expressing controls. $n = 3$–7. Due to varying overexpression levels of DOT1L, one-sample *t* test was performed using the log 2 fold change. Confidence level of 95% and a hypothetical control value of 0 were set. For all data *p*-value: *, $p < .05$; **, $p < .01$; ***, $p < .001$. Abbreviation: ER, endoplasmic reticulum.

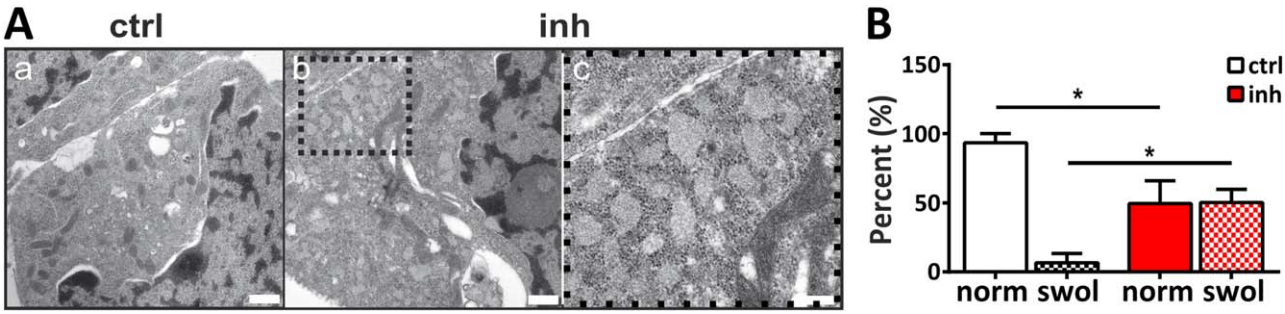

Figure 3. Morphological analyses using electron microscopy revealed swollen endoplasmic reticulum (ER) after DOT1L inhibition. **(A)**: Electron microscopy (EM) of (a) one representative cortical cell displaying normal morphology with regard to the nucleus and cytoplasmic organelles under control condition, whereas (b) signs of swollen ER were specifically observed after DOT1L inhibition. (c): Inset in b is represented at higher magnification to indicate the swollen ER after inhibition of DOT1L activity. Scale bars in a and b = 500 nm, in c = 250 nm. **(B)**: Percentage of cells containing normal (norm) or swollen (swol ER in control and DOT1L-inhibited condition as revealed by EM). Unpaired Student's *t* test, $n = 3$. *p*-Value: *, $p < .05$.

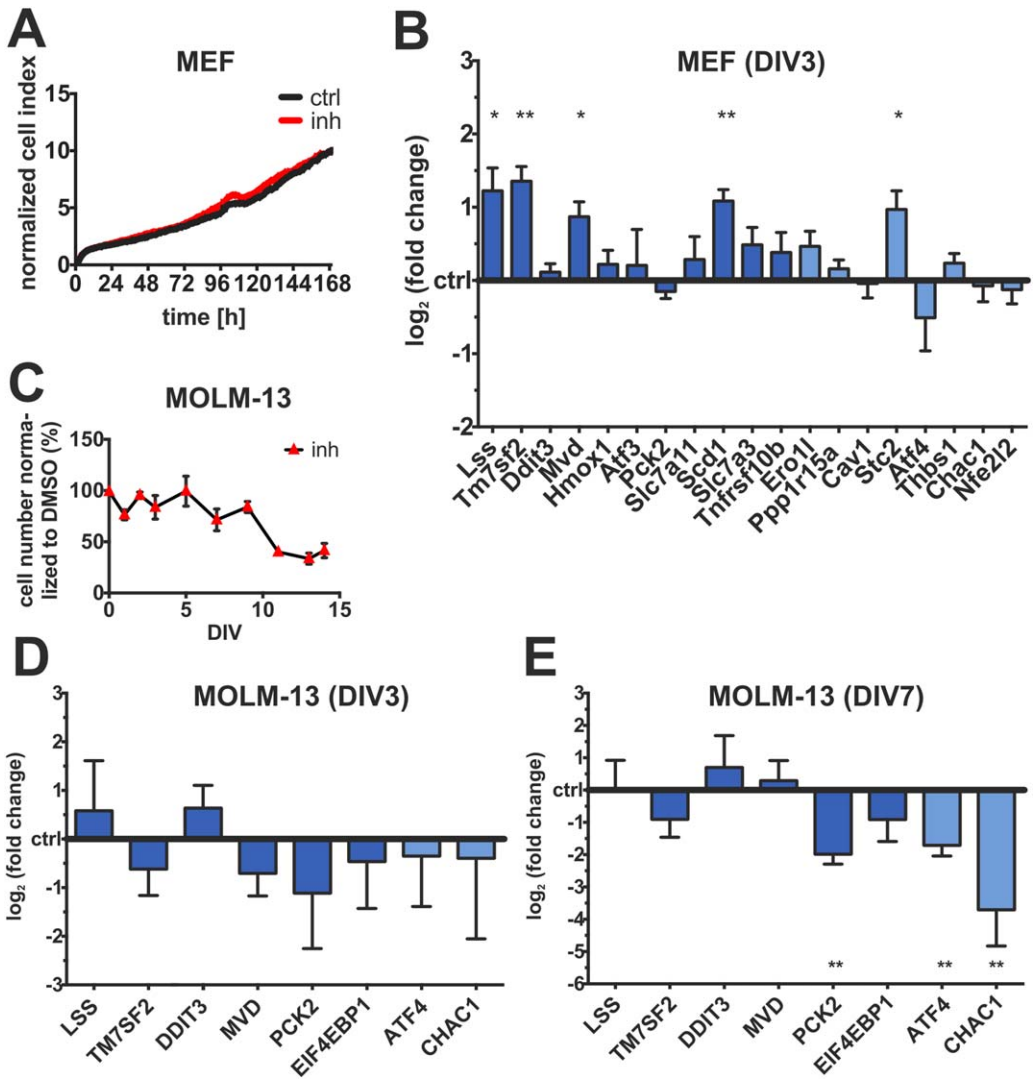

Figure 4. Transcriptional regulation of endoplasmic reticulum (ER) stress genes through DOT1L activity was cell-type specific. **(A)**: Representative graphs of real-time cell analysis revealed that inhibition of DOT1L activity did not change proliferation/survival of MEFs. One of three independent experiments is shown. **(B)**: qRTPCR validation of transcriptional alterations after DOT1L inhibition revealed increased transcription of a subset of lipid metabolism genes, but it did not activate the ER stress transcriptional program in MEFs. Log 2 of the fold change is given compared to DMSO control. Unpaired Student's *t* test, $n = 3$. **(C)**: Long-term DOT1L inhibition of MOLM-13 cells led to increased cell death. The total cell number was normalized to the DMSO control. **(D)**: Short-term inhibition of DOT1L (DIV3) of MOLM-13 cells did not change transcription of genes involved in lipid metabolism or ER stress as revealed by qRTPCR. Data represented as in (B). Unpaired Student's *t* test, $n = 3$. **(E)**: Long-term inhibition of DOT1L (DIV7) led to impaired transcription of a small number of genes implicated in ER stress. Data represented as in (B). Unpaired Student's *t* test, $n = 3$. For all data *p*-value: *, $p < .05$; **, $p < .01$. Abbreviation: MEF, mouse embryonic fibroblasts.

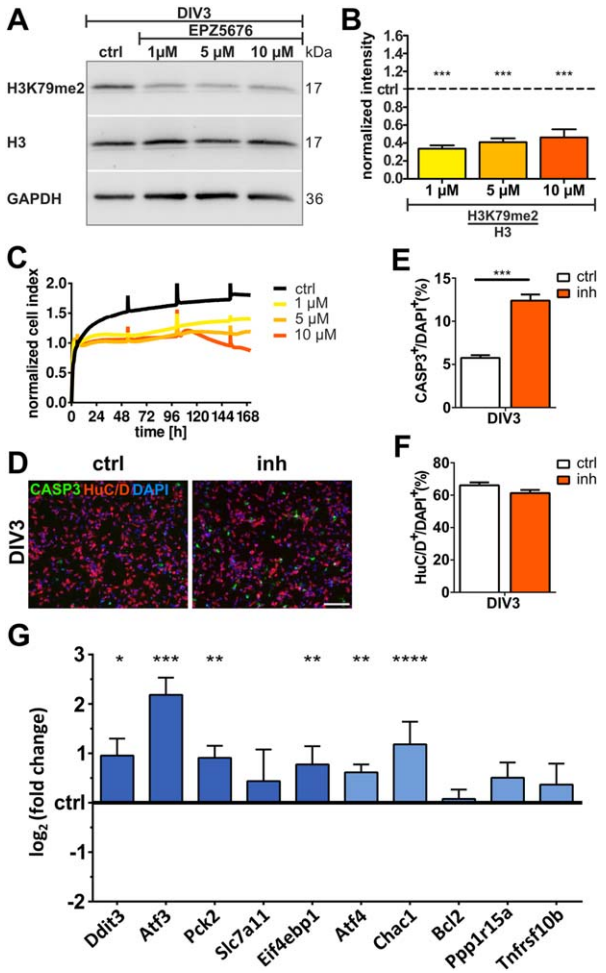

Figure 5. DOT1L inhibition using EPZ5676 corroborates impaired neural stem cell (NSC) proliferation, survival, and transcriptional activation of endoplasmic reticulum (ER) stress genes. **(A)**: Immunoblot revealed decreased H3K79me2 levels in E14.5-derived cortical NSCs after DOT1L inhibition through EPZ5676. **(B)**: Densitometric quantification of (A). Statistical evaluation was performed using one-way ANOVA followed by Student-Newman-Keuls post hoc test, $n = 5$. **(C)**: Representative graphs of real-time cell analysis of one out of five experiments showing that inhibition of DOT1L activity through EPZ5676 led to decreased proliferation and/or survival of E14.5-derived cortical NSCs in a concentration-dependent manner. **(D)**: Immunocytochemical stainings of activated Caspase3- (CASP3) and HuC/D-positive cells at DIV3 under control (ctrl, DMSO) and DOT1L-inhibited (inh) condition using 10 μM EPZ5676. Scale bar = 100 μm. **(E, F)**: Quantification of cell numbers indicated increased cell death (CASP3) but normal neuronal differentiation after interference with DOT1L activity using 10 μM EPZ5676. The number of positive cells was normalized to the total number of DAPI-positive cells. Unpaired Student's t test, $n = 4$. **(G)**: Inhibition of DOT1L using 10 μM EPZ5676 and validation of expression changes of selected genes involved in ER stress response using qRTPCR. Given is the log 2 fold change for DOT1L-inhibited samples compared to DMSO-treated controls, indicating that using EPZ5676 to interfere with DOT1L activity resulted also in increased transcription of ER stress genes. Unpaired Student's t test, $n = 4$–6. For all data p-value: *, $p < .05$; **, $p < .01$; ***, $p < .001$; ****, $p < .0001$.

on *Atf4* in MEFs and NSCs. While mouse *Atf4* is expressed stronger in NSCs after DOT1L inhibition, MEFs showed no change in its transcription. In contrast, human leukemic MOLM-13 cells responded with a significant suppression of *ATF4* transcription. Furthermore, DOT1L inhibition mostly activated transcription in cortical NSCs although many reports refer to H3K79 methylation as an activating histone modification. Interestingly, the transcriptomes of retinoic acid-treated, differentiating ESCs, as well as of induced pluripotent stem cells (iPSC) and of intestinal stem cells also revealed more genes which were activated upon loss of DOT1L expression than genes whose expression decreased [9, 14, 15]. Together with our data, these findings indicate that DOT1L might have an important, previously unanticipated role in suppressing gene expression in a context-dependent manner.

However, the view of H3K79 methylation as repressive modification might also not reflect the truth. Integrating both observations might be the conclusion that H3K79 methylation is enriched at transcriptionally active genes but it might limit their transcription to a basal level. Decreased levels of H3K79 methylation would in this case be required for stronger or full activation of transcription. This conclusion parallels the observation that interference with the H2Bub1-mediating ligase RNF20 results in relatively equal numbers of upregulated and downregulated genes despite a clear correlation between H2Bub1 levels and gene transcription [32–34]. However, H2Bub1 is a highly dynamic mark and it may confer low transcription rates, within a chromatin environment that poises genes for rapid activation, as suggested recently by Shema et al. [32]. In contrast, H3K79 methylation might be a more inert mark implicated in balancing a distinct transcriptional status, because an H3K79-specific demethylase has not been identified so far. We observed that the induction of *Atf4* and *Ddit3* was only apparent after long-term inhibition of DOT1L. This might reflect a slow turnover of H3K79 methylation at genes with a pivotal role in either differentiation or cell death. However, much more research on the impact of H3K79me2 on transcription in different microenvironments is needed to clarify these hypotheses.

Cell death follows the UPR and unresolved ER stress. Stem cells are either long-lived because of their capacity to self-renew, or they go through multiple cell divisions before they differentiate. Both conditions can predispose stem cells to increased rates of stress stimuli such as reactive oxygen species, limited amounts of nutrients, and DNA damage. Thus, although UPR and ER stress have not yet been studied extensively in stem cells, several data implicate pivotal roles. For example, *Atf4*-deficient mice show fewer hematopoietic progenitor cells in the liver, and *Atf4*-null MEFs display a defect in cell cycle progression [35]. Interestingly, HSCs and their closely related progenitors respond differently to ER stress inducers. Under stress conditions, HSCs, but not other hematopoietic progenitor cells, undergo apoptosis via activation of the *Atf4/Ddit3*-mediated transcriptional program [36].

Moreover, activation of the ER stress response is not only a mechanism for elimination of stem cells that encounter insults during development. Instead, activation of the ER stress program, for example, of *Atf4* and *Ddit3*, might also be beneficial in directing stem cells into differentiation or to maintain a proliferative status [37–40]. This indicates that the UPR has to be tightly regulated and adapted to the various cellular needs to balance cell fate decisions ranging from differentiation to cell death. Our data establish a transcriptional control of the *Atf4* and *Ddit3* ER stress genes by DOT1L and uncover a new role for chromatin modifying enzymes in regulating ER stress. We observed a broad activation of different hallmarks of ER stress. These include activation of different

transcription factors (*Atf4, Atf3, Ddit3*, and *Nfe2l2*), proteins involved in apoptosis (*Bcl2* and *Tnfrsf10b/Dr5*), in lipid or cholesterol homeostasis (*Lss, Mvd, Tm7sf2, Hmox1, Scd1*), in regulation of the redox status (*Ero1l, Slc7a11/xCT,* and *Chac1*), or in protein synthesis (*Eif4Ebp1* and *Slc7a3*). The ChIP-seq profiles of H3K79me2 revealed that most of the transcriptional changes might not be triggered directly by DOT1L, but rather occur as downstream effects. DOT1L and H3K79me2 are likely to be central regulators of the initiation of the ER stress transcription factor cascade centered on *Atf4* and *Ddit3*. Both genes are sensitive to DOT1L activity and their expression levels correlate inversely with H3K79me2 over the entire gene. The ChIP-seq profiles and the kinetics of transcriptional induction after different durations of DOT1L inhibition indicated that ATF4 might act upstream of *Ddit3* in NSCs, although *Ddit3* expression is also sensitive to H3K79me2 itself. However, *Atf4* transcription increased already 24 hours after DOT1L inhibition, which was also accompanied by an increase at the protein level. In contrast, increased transcription of *Ddit3* was observed only after 3 DIV, which might argue in favor of ATF4-dependent transcription. Important downstream targets of ATF4 are *Ddit3* [41], *Gadd34/Ppp1r15a*, and *Atf3* [30]. H3K79me2 was not enriched over *Atf3* and transcription of the latter might therefore be regulated mainly by ATF4 and/or other factors. *Ddit3* and *Gadd34/Ppp1r15a* displayed mild enrichment and both H3K79me2 as well as ATF4 could therefore influence their increased expression levels. *Bcl2, Gadd34/Ppp1r15a, Dr5/Tnfrsf10b*, and *Ero1l* are direct targets of DDIT3 [30]. Among these, *Gadd34/Ppp1r15a* and *Ero1l* were also enriched for H3K79me2 and might also be influenced directly by DOT1L. *Bcl2* was not affected on a transcriptional level in NSCs and its reduced protein level might be indicative for the activation of the apoptotic program.

Thapsigargin treatment results in ER stress in HepG2 liver carcinoma cell lines and subsequent accumulation of H3K4me3 and H3K79me2 over several transcription factors, including *DDIT3* [42]. Increased levels of H3K79me2 appear under acute stress conditions in a time frame of 1–8 hours and correlate with increased transcription. Our results did not indicate transcriptional activation of *Ddit3* after short-term inhibition of DOT1L. Only long-term treatment induced *Ddit3* transcription, which was accompanied by decreased levels of H3K79me2. These results are further consistent with a context-dependent mode of H3K79me2-mediated transcriptional control that differs between NSCs and other cell systems. It also indicates a cell and/or context-dependent regulation of the ER stress response.

Further data report on the implication of histone modifying enzymes in the control of ER stress. The MLL protein family mediates H3K4me3 and MLL activity is also present at the

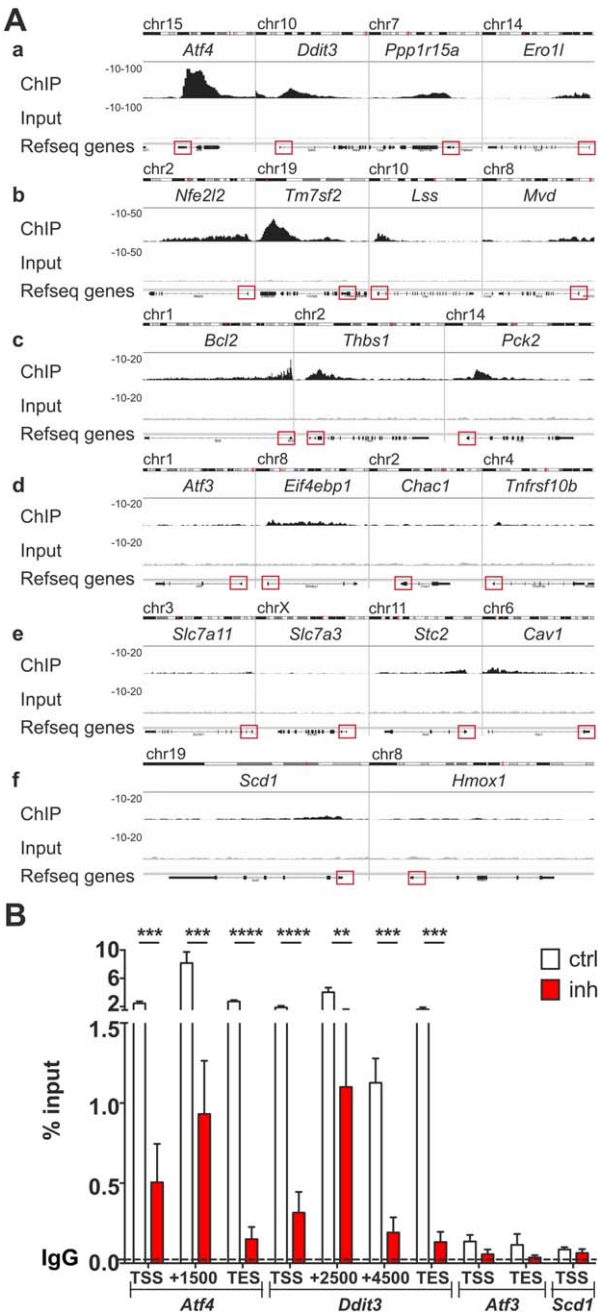

Figure 6. DOT1L-mediated H3K79me2 interfered with expression of central endoplasmic reticulum (ER) stress transcription factors *Atf4* and *Ddit3*. **(A)**: Representative ChIP-seq reads of H3K79me2 from E14.5-derived cortical cells for 21 genes implicated in ER stress response, mapped to the mm9 genome assembly. Integrative genome viewer was used to visualize the H3K79me2 enrichment. Given are the H3K79me2 ChIP samples (1st lane), the input samples (2nd lane), both as merged data from two independent experiments, and gene positions defined by RefSeq (3rd lane). A red box highlights the first exon including the TSS. (a): H3K79me2 was highly enriched at the TSS and the gene body of *Atf4* and *Ddit3. Ppp1r15a* and *Ero1l* also showed enrichment, but not as strong as compared to the former. Scaling: −10 to 200 RPKM. (b): *Nfe2l2, Tm7sf2, Lss*, and *Mvd* displayed moderate H3K79me2 enrichment. Scaling: −10 to 100 RPKM. (c): *Bcl2, Thbs1*, and *Pck2* showed slight H3K79me2 enrichment. Scaling: −10 to 25 RPKM. (d–f): *Atf3, Eif4ebp1, Chac1, Tnfrsf10b, Slc7a11, Slc7a3, Stc2, Cav1, Scd1*, and *Hmox1* did show minor or no enrichment for H3K79me2. Scaling: −10 to 25 RPKM. **(B)**: Interference with DOT1L activity confirmed reduced H3K79me2 enrichment at the TSS, gene body, and TES of *Atf4* and *Ddit3* using ChIP and qRTPCR in this condition compared to the control. DOT1L inhibition did not affect H3K79me2 status at the gene loci studied for *Atf3* and *Scd1*. Results are represented as % input. IgG was used as negative control and the mean is depicted as dashed line. Two-way ANOVA and Šidák multicomparison test, $n = 3$. *p*-Value: **, $p < .01$; ***, $p < .001$; ****, $p < .0001$. Abbreviations: ChIP, chromatin immunoprecipitation; TES, transcriptional end site; TSS, transcriptional start site.

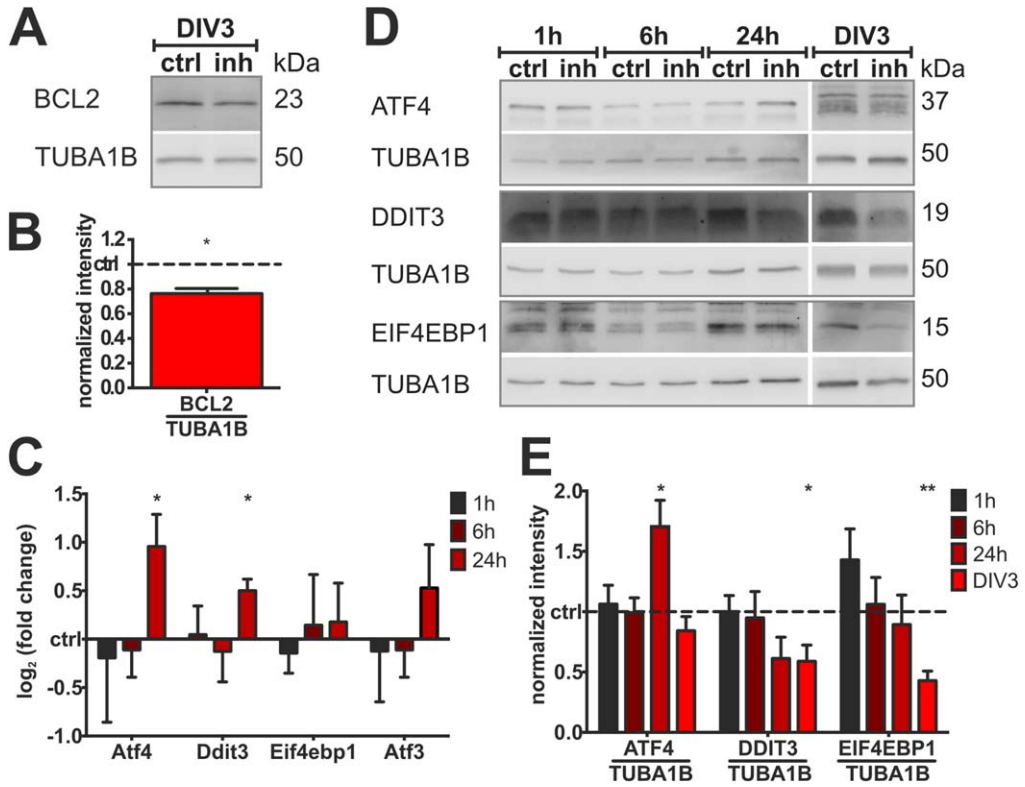

Figure 7. Chronic inhibition of DOT1L induced transcription and translation of endoplasmic reticulum (ER) stress genes. **(A)**: Reduced DOT1L activity led to decreased levels of BCL2-protein at DIV3 in E14.5-derived cortical neural stem cells (NSCs) as revealed by immunoblotting. **(B)**: Densitometric quantification of immunoblots for BCL2 and TUBA1B. One-sample *t* test with confidence level of 95% and hypothetical value of 1, $n = 3$. **(C)**: Short-term inhibition of DOT1L (1 hour and 6 hours) did not change transcription of genes involved in ER stress. Interference with DOT1L activity for 24 hours led to increased expression of *Atf4* and *Ddit3* as validated by qRTPCR. Log 2 fold change is given compared to DMSO control. Unpaired Student's *t* test, $n = 3$–4. **(D)**: Immunoblot of proteins extracted after different time points (1 hour, 6 hours, 24 hours, DIV3) of DOT1L inhibition from E14.5-derived cortical NSCs which were probed for ATF4, DDIT3, and EIF4EBP1. **(E)**: Densitometric quantification of (D) revealed no significant alteration in protein expression of ER stress genes after short-term DOT1L inhibition (1 hour and 6 hours). Increased levels of ATF4 protein appeared after 24 hours DOT1L inhibition. DDIT3 and EIF4EBP1 protein levels significantly decreased at DIV3. Quantification as in (B), $n = 3$–4. *p*-Value: *, $p < .05$; **, $p < .01$.

promoters of genes implicated in the homeostasis of glycoproteins in the ER [43] as well as at the promoters of *GPR78* and *DDIT3* [44]. In this context, transcription of ER stress genes *GPR78* and *DDIT3* depends not only on H3K4me3, but further data show that the SAGA (Spt-Ada-Gcn5-acetyltransferase)-associated factor 29 (SGF29) binds to H3K4me3, and recruits the SAGA complex with its H3K14 histone acetylation activity. Accordingly, loss of SGF29 results in decreased cell survival alongside with decreased H3K4me3, H3K14ac, and transcription of *GPR78* and *DDIT3* [44]. Thus, ER stress gene promoters are marked with H3K4me3 that renders them susceptible for adapted transcriptional activation upon stress insults.

Interestingly, DOT1L might affect ER stress on multiple levels through its interaction partner BAT3/BAG6. BAT3 interaction with DOT1L is implicated in H3K79me2 and formation of TRP53BP1-associated DSB repair foci [45]. In addition, BAT3 is localized at the ER membrane and prevents aggregation of misfolded protein substrates that are transported to the proteasome for degradation [46].

Our findings that DOT1L is implicated in the regulation of the ER stress response in NSCs might also be of clinical relevance because ER stress and the UPR are implicated in neurodegenerative diseases. Amyloid-β induces local translation of *Atf4* in axons, but not its nuclear transcription. This induces ER stress and subsequent neurodegeneration, indicating a role for *Atf4* in Alzheimer's disease [47]. Accumulation of misfolded proteins such as amyloid-β, α-synuclein, and huntingtin is associated with the pathologies of Alzheimer's, Parkinson's, and Huntington's diseases, respectively. Several lines of research suggest that activation of *Ddit3* might be involved in these pathologies [41]. In addition, ER stress, protein aggregation, and induction of *Ddit3*-transcription were observed after global cerebral ischemia [48]. These observations support a potential association of the loss of DOT1L activity with neurodegenerative diseases, or that its activity could be neuroprotective by preventing initiation of the ER stress program. Although we did not observe increased cell death in mature neurons after DOT1L inhibition, DOT1L activity might be protective under conditions where neurons have to cope with insults such as hypoxia, inflammation, or accumulation of unfolded proteins by delaying an ER stress response.

Lower levels of H3K79me2 have been observed in patients presenting with NTDs [21]. NTDs are also an outcome of diabetic embryopathy which might also be associated with ER stress [49]. It is thus conceivable, albeit speculative, that ER stress in response to decreased levels of H3K79me2 through impaired DOT1L activity might also be causative in the NTD pathology.

Conclusions

We conclude from these data that the crosstalk between different posttranslational histone modifications, including H3K4me3, H3K14ac, and H3K79me2, may provide a molecular mechanism to fine tune transcriptional activation of ER stress genes. Combinations of different histone modifications might allow the cell to activate the protective or the final death pathway. In this context, it seems that loss of H3K79me2 at the *Atf4* and *Ddit3* promoters marks a point-of-no-return that activates the death program, at least in NSCs.

Acknowledgments

This work was supported by The Deutsche Forschungsgemeinschaft and the CRC992 Medical Epigenetics through a grant to T.V. (A03). ChIP-seq was performed through a grant to R. Backofen and T. Manke of the CRC992 (Z01). We thank P.J. Brown (University of Toronto) for providing SGC0946, D. Pfeiffer (Medicine I, University Clinic Freiburg) for microarray analyses, BIOSS Toolbox (Centre for Biological Signalling Studies, University of Freiburg) for plasmids, and J. Pruszak, J. Neumann, M. Ell, F. Ipek, M. Loeffler, and E. Gimbel (Mol. Embryology, University of Freiburg) for technical advice and/or assistance.

Author Contributions

D.R. and N.H.: collection and/or assembly of data, data analysis and interpretation, and manuscript writing; P.B.: collection and/or assembly of data and manuscript writing; A.V.: collection and/or assembly of data and data analysis and interpretation; S.H., S.N., B.G., and U.B.: collection and/or assembly of data; T.V.: conception and design, financial support, collection and/or assembly of data, data analysis and interpretation, and manuscript writing. D.R., N.H., and P.B. contributed equally to this article.

Disclosure of Potential Conflicts of Interest

The authors indicate no potential conflicts of interest.

References

1 Takahashi Y-H, Schulze JM, Jackson J et al. Dot1 and histone H3K79 methylation in natural telomeric and HM silencing. Mol Cell 2011;42:118–126.
2 Tatum D, Li S. Evidence that the histone methyltransferase Dot1 mediates global genomic repair by methylating histone H3 on lysine 79. J Biol Chem 2011;286:17530–17535.
3 Huyen Y, Zgheib O, Ditullio RA et al. Methylated lysine 79 of histone H3 targets 53BP1 to DNA double-strand breaks. Nature 2004;432:406–411.
4 Oksenych V, Zhovmer A, Ziani S et al. Histone methyltransferase DOT1L drives recovery of gene expression after a genotoxic attack. PLoS Genet 2013;9:e1003611.
5 Kim W, Kim R, Park G et al. The deficiency of H3K79 histone methyltransferase DOT1L inhibits cell proliferation. J Biol Chem 2012;287:5588–5599.
6 Ontoso D, Acosta I, van Leeuwen F et al. Dot1-dependent histone H3K79 methylation promotes activation of the Mek1 meiotic checkpoint effector kinase by regulating the Hop1 adaptor. PLoS Genet 2013;9:e1003262.
7 Kim W, Choi M, Kim J-E. The histone methyltransferase Dot1/DOT1L as a critical regulator of the cell cycle. Cell Cycle 2014;13:726–738.
8 Jones B, Su H, Bhat A et al. The histone H3K79 methyltransferase Dot1L is essential for mammalian development and heterochromatin structure. PLoS Genet 2008;4:e1000190.
9 Barry ER, Krueger W, Jakuba CM et al. ES cell cycle progression and differentiation require the action of the histone methyltransferase Dot1L. Stem Cells 2009;27:1538–1547.
10 Cattaneo P, Kunderfranco P, Greco C et al. DOT1L-mediated H3K79me2 modification critically regulates gene expression during cardiomyocyte differentiation. Cell Death Differ 2014 [Epub ahead of print].
11 Nguyen AT, Xiao B, Neppl RL et al. DOT1L regulates dystrophin expression and is critical for cardiac function. Genes Dev 2011;25:263–274.
12 Feng Y, Yang Y, Ortega MM et al. Early mammalian erythropoiesis requires the Dot1L methyltransferase. Blood 2010;116:4483–4491.
13 Jo SY, Granowicz EM, Maillard I et al. Requirement for Dot1l in murine postnatal hematopoiesis and leukemogenesis by MLL translocation. Blood 2011;117:4759–4768.
14 Ho L-L, Sinha A, Verzi M et al. DOT1L-mediated H3K79 methylation in chromatin is dispensable for Wnt pathway-specific and other intestinal epithelial functions. Mol Cell Biol 2013;33:1735–1745.
15 Onder TT, Kara N, Cherry A et al. Chromatin-modifying enzymes as modulators of reprogramming. Nature 2012;483:598–602.
16 Kim S-K, Jung I, Lee H et al. Human histone H3K79 methyltransferase DOT1L protein [corrected] binds actively transcribing RNA polymerase II to regulate gene expression. J Biol Chem 2012;287:39698–39709.
17 Buttner N, Johnsen SA, Kügler S et al. Af9/Mllt3 interferes with Tbr1 expression through epigenetic modification of histone H3K79 during development of the cerebral cortex. Proc Natl Acad Sci USA 2010;107:7042–7047.
18 Zhang W, Xia X, Reisenauer MR et al. Dot1a-AF9 complex mediates histone H3 Lys-79 hypermethylation and repression of ENaCalpha in an aldosterone-sensitive manner. J Biol Chem 2006;281:18059–18068.
19 Mohan M, Herz HM, Takahashi Yh et al. Linking H3K79 trimethylation to Wnt signaling through a novel Dot1-containing complex (DotCom). Genes Dev 2010;24:574–589.
20 Park G, Gong Z, Chen J et al. Characterization of the DOT1L network: Implications of diverse roles for DOT1L. Protein J 2010;29:213–223.
21 Zhang Q, Xue P, Li H et al. Histone modification mapping in human brain reveals aberrant expression of histone H3 lysine 79 dimethylation in neural tube defects. Neurobiol Dis 2013;54:404–413.
22 Sabra M, Texier P, El Maalouf J et al. The Tudor protein survival motor neuron (SMN) is a chromatin-binding protein that interacts with methylated lysine 79 of histone H3. J Cell Sci 2013;126:3664–3677.
23 Vogel T, Ahrens S, Buttner N et al. Transforming growth factor promotes neuronal cell fate of mouse cortical and hippocampal progenitors in vitro and in vivo: Identification of Nedd9 as an essential signaling component. Cereb Cortex 2010;20:661–671.
24 Langmead B, Salzberg SL. Fast gapped-read alignment with Bowtie 2. Nat Methods 2012;9:357–359.
25 Zhang Y, Liu T, Meyer CA et al. Model-based analysis of ChIP-Seq (MACS). Genome Biol 2008;9:R137.
26 Yu W, Chory EJ, Wernimont AK et al. Catalytic site remodelling of the DOT1L methyltransferase by selective inhibitors. Nat Commun 2012;3:1288.
27 McGinty RK, Kim J, Chatterjee C et al. Chemically ubiquitylated histone H2B stimulates hDot1L-mediated intranucleosomal methylation. Nature 2008;453:812–816.
28 Daigle SR, Olhava EJ, Therkelsen CA et al. Selective killing of mixed lineage leukemia cells by a potent small-molecule DOT1L inhibitor. Cancer Cell 2011;20:53–65.
29 Daigle SR, Olhava EJ, Therkelsen CA et al. Potent inhibition of DOT1L as treatment of MLL-fusion leukemia. Blood 2013;122:1017–1025.
30 Sano R, Reed JC. ER stress-induced cell death mechanisms. Biochim Biophys Acta 2013;1833:3460–3470.
31 Wang CM, Tsai SN, Yew TW et al. Identification of histone methylation multiplicities patterns in the brain of senescence-accelerated prone mouse 8. Biogerontology 2009;11:87–102.
32 Shema E, Tirosh I, Aylon Y et al. The histone H2B-specific ubiquitin ligase RNF20/hBRE1 acts as a putative tumor suppressor through selective regulation of gene expression. Genes Dev 2008;22:2664–2676.
33 Minsky N, Shema E, Field Y et al. Monoubiquitinated H2B is associated with the transcribed region of highly expressed genes in human cells. Nat Cell Biol 2008;10:483–488.

34 Pavri R, Zhu B, Li G et al. Histone H2B monoubiquitination functions cooperatively with FACT to regulate elongation by RNA polymerase II. Cell 2006;125:703–717.
35 Masuoka HC, Townes TM. Targeted disruption of the activating transcription factor 4 gene results in severe fetal anemia in mice. Blood 2002;99:736–745.
36 van Galen P, Kreso A, Mbong N et al. The unfolded protein response governs integrity of the haematopoietic stem-cell pool during stress. Nature 2014;510:268–272.
37 Cho YM, Jang YS, Jang YM et al. Induction of unfolded protein response during neuronal induction of rat bone marrow stromal cells and mouse embryonic stem cells. Exp Mol Med 2009;41:440–452.
38 Kawada K, Iekumo T, Saito R et al. Aberrant neuronal differentiation and inhibition of dendrite outgrowth resulting from endoplasmic reticulum stress. J Neurosci Res 2014;92:1122–1133.
39 Yu S, Zhu K, Lai Y et al. atf4 promotes β-catenin expression and osteoblastic differentiation of bone marrow mesenchymal stem cells. Int J Biol Sci 2013;9:256–266.
40 Alter J, Bengal E. Stress-induced C/EBP homology protein (CHOP) represses MyoD transcription to delay myoblast differentiation. PLoS One 2011;6:e29498.
41 Oyadomari S, Mori M. Roles of CHOP/GADD153 in endoplasmic reticulum stress. Cell Death Differ 2004;11:381–389.
42 Donati G, Imbriano C, Mantovani R. Dynamic recruitment of transcription factors and epigenetic changes on the ER stress response gene promoters. Nucleic Acids Res 2006;34:3116–3127.
43 Wang X, Ju L, Fan J et al. Histone H3K4 methyltransferase Mll1 regulates protein glycosylation and tunicamycin-induced apoptosis through transcriptional regulation. Biochim Biophys Acta 2014;1843:2592–2602.
44 Schram AW, Baas R, Jansen PWTC et al. A dual role for SAGA-associated factor 29 (SGF29) in ER stress survival by coordination of both histone H3 acetylation and histone H3 lysine-4 trimethylation. PLoS One 2013;8:e70035.
45 Wakeman TP, Wang Q, Feng J et al. Bat3 facilitates H3K79 dimethylation by DOT1L and promotes DNA damage-induced 53BP1 foci at G1/G2 cell-cycle phases. EMBO J 2012;31:2169–2181.
46 Xu Y, Liu Y, Lee J-g et al. A ubiquitin-like domain recruits an oligomeric chaperone to a retrotranslocation complex in endoplasmic reticulum-associated degradation. J Biol Chem 2013;288:18068–18076.
47 Baleriola J, Walker CA, Jean YY et al. Axonally synthesized ATF4 transmits a neurodegenerative signal across brain regions. Cell 2014;158:1159–1172.
48 Paschen W, Gissel C, Linden T et al. Activation of gadd153 expression through transient cerebral ischemia: Evidence that ischemia causes endoplasmic reticulum dysfunction. Brain Res Mol Brain Res 1998;60:115–122.
49 Zhao Z, Eckert RL, Reece EA. Reduction in embryonic malformations and alleviation of endoplasmic reticulum stress by nitric oxide synthase inhibition in diabetic embryopathy. Reprod Sci 2012;19:823–831.


See www.StemCells.com for supporting information available online.

